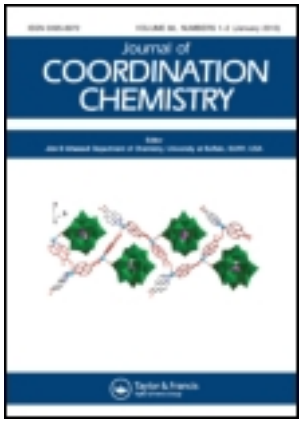

Journal of Coordination Chemistry
Publication details, including instructions for authors and subscription information:
http://www.tandfonline.com/loi/gcoo20

Syntheses, structures, and nonlinear optical properties of two polynuclear homometallic and heterometallic cluster compounds containing silver(I) bromide species

Hua-Tian Shi[a], Lu-Jun Zhou[b], Ai-Quan Jia[a], Qun Chen[b] & Qian-Feng Zhang[abc]

[a] Institute of Molecular Engineering and Applied Chemistry, Anhui University of Technology, Ma'anshan, P.R. China

[b] Department of Applied Chemistry, School of Petrochemical Engineering, Changzhou University, Jiangsu, P.R. China

[c] Coordination Chemistry Institute, Nanjing University, Nanjing, P.R. China

Accepted author version posted online: 07 Oct 2013.Published online: 15 Nov 2013.

To cite this article: Hua-Tian Shi, Lu-Jun Zhou, Ai-Quan Jia, Qun Chen & Qian-Feng Zhang (2013) Syntheses, structures, and nonlinear optical properties of two polynuclear homometallic and heterometallic cluster compounds containing silver(I) bromide species, Journal of Coordination Chemistry, 66:21, 3740-3748, DOI: 10.1080/00958972.2013.851380

To link to this article: http://dx.doi.org/10.1080/00958972.2013.851380

Journal of Coordination Chemistry, 2013
Vol. 66, No. 21, 3740–3748, http://dx.doi.org/10.1080/00958972.2013.851380

Syntheses, structures, and nonlinear optical properties of two polynuclear homometallic and heterometallic cluster compounds containing silver(I) bromide species

HUA-TIAN SHI†, LU-JUN ZHOU‡, AI-QUAN JIA†, QUN CHEN‡ and QIAN-FENG ZHANG*†‡§

†Institute of Molecular Engineering and Applied Chemistry, Anhui University of Technology, Ma'anshan, P.R. China
‡Department of Applied Chemistry, School of Petrochemical Engineering, Changzhou University, Jiangsu, P.R. China
§Coordination Chemistry Institute, Nanjing University, Nanjing, P.R. China

(*Received 20 May 2013; accepted 28 August 2013*)

Interaction of $[Et_4N]_2[WSe_4]$ and AgBr in the presence of $[Et_4N]Br{\cdot}xH_2O$ in a DMF/MeCN/2-picoline solution (3 : 2 : 1) at room temperature afforded a colorless crystalline compound $[Et_4N]_6[(AgBr)_6(\mu_3\text{-}Br)_2(\mu_4\text{-}Br)_3]Br$ (**1**) in 21% yield and a red crystalline compound $[Et_4N]_4[(\mu_5\text{-}WSe_4)(AgBr)_5(\mu\text{-}Br)_2]$ (**2**) in 48% yield. The cluster anion in **1** comprises six AgBr fragments bridged by three bromides and capped by two bromides, forming a trigonal prism structure. The cluster anion in **2** consists of five AgBr fragments coordinated to five edges of the tetrahedral $[WSe_4]^{2-}$ along with two bridging bromides connected to each of the two pairs of symmetric silvers, exhibiting a crown-like core structure. The nonlinear optical absorption and refraction of **2** were determined to be $\alpha_2 = 5.72 \times 10^{-9}$ m W^{-1} and $n_2 = 3.64 \times 10^{-9}$ esu, respectively.

Keywords: Silver; Polynuclear cluster; Selenide cluster; Synthesis; Optical nonlinearity

1. Introduction

Since the cubic cage-shaped clusters $(n\text{-}Bu_4N)_3[MoS_4Ag_3BrX_3]$ (X = Cl and I) exhibited strong optical limiting capability in 1994 [1], continuous advances in the syntheses of heterothiometallic silver-containing clusters have been stemming from intriguing structural features and optical properties [2, 3]. For example, the hexagonal prism cage-shaped, polymeric, and polynuclear argentothiometallic clusters display strong nonlinear optical behavior [4–7]. Structure-property relationships have also been extended to the analogous heteroselenometallic clusters [8]. An important reason is due to the nonlinearity improvement of this class of clusters arising from the fact that the silver-containing clusters have much lower pump energy, which probably originates from the heavy atom effect existing in scattering-induced nonlinearity [9, 10]. Smolentsev has reported the preparation of a

*Corresponding author. Email: zhangqf@ahut.edu.cn

tungsten–selenium cluster $Cs_3Na_2[W_3Se_4(CN)_9]\cdot 0.5Et_4NBr\cdot 5H_2O$ by W(II)–W(IV) conversion in solution [11] and Jin has reported a W–Se–Ir cluster by reaction of Cp* Ir $[Se_2C_2(B_{10}H_{10})]$ with $[W(CO)_3(py)_3]$ in the presence of $BF_3\cdot OEt_2$ [12], which may provide an alternate way to synthesize heterometallic tungsten–selenium clusters. We have long-standing interest in the heteroselenometallic clusters formed from reactions of $[MSe_4]^{2-}$ and coinage metal species, of which the argentoselenometallic clusters are promising candidates of optical limiting materials among all the selenometallic clusters studied [13–15]. Neutral polynuclear argentoselenometallic clusters with σ-donating phosphines exhibit good photo-stability and relatively stable optical limiting effects [15]. Thus, the strategy of this project is directed towards searching for new optical inorganic cluster materials. With this in mind, we are continuing to explore reaction of the tetraselenometallic anions and the silver-containing species. Reaction of $[Et_4N]_2[WSe_4]$ and AgBr in the presence of $[Et_4N]Br\cdot xH_2O$ was carried out, resulting in isolation of two hexanuclear clusters $[Et_4N]_6[(AgBr)_6(\mu_3\text{-}Br)_2(\mu_4\text{-}Br)_3]Br$ (**1**) with a trigonal prism core structure and $[Et_4N]_4[(\mu_5\text{-}WSe_4)(AgBr)_5(\mu\text{-}Br)_2]$ (**2**) with a crown-like core structure. The syntheses and structures along with the nonlinear optical properties of **2** are reported in this article.

2. Experimental

2.1. *General*

All manipulations were conducted using Schlenk techniques under an atmosphere of nitrogen. $[Et_4N]_2[WSe_4]$ was prepared by modification of the literature method [16]. AgBr and $[Et_4N]Br\cdot xH_2O$ were purchased from Alfa Aesar Ltd. and used without purification. All elemental analyzes were carried out using a Perkin–Elmer 2400 CHN analyzer. Infrared spectra were measured on a Digilab FTS-40 spectrophotometer with pressed KBr pellets. Electronic absorption spectra were obtained on a Hitachi U-3410 spectrophotometer.

2.2. *Syntheses of $[Et_4N]_6[(AgBr)_6(\mu_3\text{-}Br)_2(\mu_3\text{-}Br)_3]Br$ (1) and $[Et_4N]_4[(\mu_5\text{-}WSe_4)(AgBr)_5(\mu\text{-}Br)_2]$ (2)*

To a suspended solution of AgBr (108 mg, 1.0 mM) and $[Et_4N]Br\cdot xH_2O$ (260 mg, 0.1 mM) in MeCN (10 mL) was added a solution of $[Et_4N]_2[WSe_4]$ (152 mg, 0.20 mM) in DMF (15 mL). The mixture was stirred at room temperature for 2 h, during which the dark red solution with red solid gradually formed. Upon addition of 5 mL of 2-picoline solution, the solid precipitate redissolved. The resultant solution was continuously stirred for an additional 4 h and filtered to give a clear, dark red filtrate. The filtrate was carefully layered with Et_2O (30 mL) at room temperature. Within five days, colorless hexagonal and red prism crystals were formed from the solution. Colorless and red crystals were separated manually and were characterized as $[Et_4N]_6[(AgBr)_6(\mu_3\text{-}Br)_2(\mu_3\text{-}Br)_3]Br$ (**1**) and $[Et_4N]_4[(\mu_5\text{-}WSe_4)(AgBr)_5(\mu\text{-}Br)_2]$ (**2**), respectively. For **1**: Yield: 48 mg, 21% (relative to silver). Anal. Calcd for $C_{48}H_{120}Ag_6Br_{12}N_6$: C, 24.15; H, 5.07; N, 3.52%. Found: C, 24.04; H, 5.02; N, 3.49%. IR (CsI, cm^{-1}): ν(C–N) 1103 (s) 982 (m), ν(Ag–Br) 419 (m). UV–vis (DMF, nm): 347 (sh), 469 (br). For **2**: Yield: 203 mg, 48% (relative to tungsen). Anal. Calcd for $C_{32}H_{80}Ag_5Br_7N_4Se_4W$: C, 18.13; H, 3.80; N, 2.64%. Found: C, 18.12; H, 3.75; N, 2.59%. IR (CsI, cm^{-1}): ν(C–N) 1101 (s) 994 (m), ν(W-Se) 314 (m). UV–vis (DMF, nm): 341 (sh), 453 (br).

2.3. *Crystal structure determination*

Crystallographic data and experimental details for **1** and **2** are summarized in table 1. Intensity data were collected on a Bruker SMART APEX 2000 CCD area-detecting diffractometer using graphite-monochromated Mo Kα radiation (λ = 0.71073 Å) at 296 (2) K. The collected frames were processed with SAINT [17]. The data were corrected for absorption using SADABS [18]. Structures were solved by direct methods and refined by full-matrix least-squares on F^2 using the SHELXTL software package [19, 20]. All non-hydrogen atoms were refined anisotropically. The positions of hydrogens were generated geometrically (C_{sp3}–H = 0.96 Å) and included in the structure factor calculations with assigned isotropic thermal parameters but were not refined. The carbons of ethyl groups of $[Et_4N]^+$ in **2** were refined isotropically with hydrogens. The largest peaks in the final difference maps had heights of 2.987 e Å^{-3} for **1** and 1.503 e Å^{-3} for **2** and are in the vicinity of the silver and tungsten, respectively.

2.4. *Optical measurements*

A DMF solution of 1.83×10^{-4} M dm^{-3} of **2** was placed in a 1 mm quartz cuvette for optical measurements. The optical limiting characteristics along with nonlinear absorption and refraction were investigated with linearly polarized laser light (λ = 532 nm, pulse width = 7 ns) generated from a Q-switched and frequency-doubled Nd:YAG laser. The spatial profiles of the optical pulses were nearly Gaussian. The laser beam was focused with a 25 cm focal length focusing mirror. The radius of the laser beam waist was measured to be 30 ± 5 μm (half-width at 1/e^2 maximum in irradiance). The incident and transmitted pulse energies were measured simultaneously by two laser precision detectors (RjP-735 energy

Table 1. Crystallographic data for **1** and **2**.

Cluster	**1**	**2**
Empirical formula	$C_{48}H_{120}Ag_6Br_{12}N_6$	$C_{32}H_{80}Ag_5Br_7N_4Se_4W$
Formula weight	2387.64	2119.41
Crystal system	Hexagonal	Monoclinic
a (Å)	19.026(7)	23.797(3)
b (Å)		10.8141(5)
c (Å)	11.938(5)	22.480(3)
β (°)		94.699(2)
V (Å^3)	3742(2)	5765.5(14)
Space group	$P6_3/m$	$C2/c$
Z	3	4
D_{Calcd} (g cm^{-3})	2.119	2.442
Temperature (K)	296(2)	296(2)
F(0 0 0)	2304	3960
M(Mo Kα) (mm^{-1})	7.979	11.055
Total refln.	10,725	17,556
Independent refln.	2993	6559
R_{int}	0.0650	0.1142
Parameters	132	169
R_1[a], wR_2[b] ($I > 2\sigma(I)$)	0.0543, 0.0907	0.0700, 0.1505
R_1, wR_2 (all data)	0.0632, 0.1161	0.1030, 0.2033
GoF[c]	0.992	0.910

[a]$R_1 = \Sigma||F_o| - |F_c||/\Sigma|F_o|$.
[b]$wR_2 = [\Sigma w(|F_o^2| - |F_c^2|)^2/\Sigma w|F_o^2|^2]^{1/2}$.
[c]$\text{GoF} = [\Sigma w(|F_o| - |F_c|)^2/(N_{obs} - N_{param})]^{1/2}$.

probes) communicating to a computer via an IEEE interface [21, 22], while the incident pulse energy was varied by a Newport Com. Attenuator. The interval between the laser pulses was chosen to be 10 s to avoid the influence of thermal and long-term effects. The details of the set-up can be found elsewhere [23, 24].

3. Results and discussion

We have previously reported crown-like heteroselenometallic clusters $[Et_4N]_4[(\mu_5\text{-}WSe_4)(CuX)_5(\mu\text{-}X)_2]$ (X = Cl, Br, I) which were prepared from reactions of $[Et_4N]_2[WSe_4]$ with CuX and $[Et_4N]X{\cdot}xH_2O$ in the presence of 2-picoline [23]. Similarly, treatment of $[Et_4N]_2[WSe_4]$ and AgBr in the presence of $[Et_4N]Br{\cdot}xH_2O$ in DMF/MeCN/2-picoline (3 : 2 : 1) at room temperature gave clear dark red solution from which two different compounds, $[Et_4N]_6[(AgBr)_6(\mu_3\text{-}Br)_2(\mu_4\text{-}Br)_3]Br$ (**1**) as colorless crystals and $[Et_4N]_4[(\mu_5\text{-}WSe_4)(AgBr)_5(\mu\text{-}Br)_2]$ (**2**) as red crystals, were obtained in 21% and 48%, respectively. The 2-picoline is a co-solvent instead of a ligand in the present system. Addition of a small amount of 2-picoline increases the solubility of the solid reactants, resulting in isolation of crystalline products in moderate yields. A similar synthetic route was also used to prepare analogous copper clusters [13, 25]. The infrared spectra of **1** and **2** display typical absorptions at 990–1100 cm^{-1}, characteristic for ν(C–N) of $[Et_4N]^+$. The strong absorption at 419 cm^{-1} in the IR spectrum of **1** may be attributed to ν(Ag–Br). The IR spectrum of **2** shows bridging W–Se vibrations at 314 cm^{-1}, lower than that for free $[WSe_4]^{2-}$ [26].

The structure of **1** was confirmed by a single-crystal X-ray diffraction. Figure 1 shows the molecular structure of $[(AgBr)_6(\mu_3\text{-}Br)_2(\mu_4\text{-}Br)_3]^{5-}$ in **1**. Table 2 lists selected bond lengths and angles. As for the iodide analog $[Et_4N]_6[Ag_6I_{11}]I$, previously reported by Hong [27], the crystal structure consists of six $[Et_4N]^+$ cations, one iodide and one hexanuclear cluster anion. The cluster anion $[(AgBr)_6(\mu_3\text{-}Br)_2(\mu_4\text{-}Br)_3]^{5-}$ comprises a prism of 6 silvers and 11 bromides. The five faces and six corners of the prism are connected to 11 bromides, forming a trigonal bipyramid. Each silver is coordinated by four bromides in a distorted tetrahedral geometry. The Br–Ag–Br angles range from 95.66(13) to 128.90(10)°. The Ag–Br–Ag angles fall in the range 68.16(18)–119.90(9)°. The average Ag···Ag and Ag–Br distances are 3.190(9) and 2.735(4) Å, respectively, of which Ag–Br bonds are

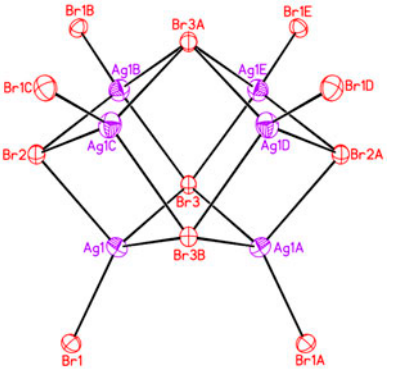

Figure 1. A perspective view of $[(AgBr)_6(\mu_3\text{-}Br)_2(\mu_3\text{-}Br)_3]^{5-}$ in **1** with the ellipsoids drawn at 40% probability.

Table 2. Selected bond lengths (Å) and angles (°) for **1**. Estimated standard deviations are given in parenthesis.

Ag(1)–Br(1)	2.540(4)	Ag(1)–Br(2)	2.750(4)
Ag(1)–Br(3)	2.803(4)	Ag(1)–Br(3)#1	2.846(4)
Ag(1)···Ag(1)#2	3.190(9)		
Br(1)–Ag(1)–Br(2)	116.17(17)	Br(1)–Ag(1)–Br(3)	121.54(7)
Br(2)–Ag(1)–Br(3)	96.66(13)	Br(1)–Ag(1)–Br(3)#1	121.95(7)
Br(2)–Ag(1)–Br(3)#1	95.66(13)	Br(3)–Ag(1)–Br(3)#1	99.23(15)
Br(1)–Ag(1)–Ag(1)#2	114.93(8)	Br(2)–Ag(1)–Ag(1)#2	128.90(10)
Ag(1)#1–Br(2)–Ag(1)	84.75(14)	Ag(1)#2–Br(3)–Ag(1)	69.35(18)
Ag(1)–Br(3)–Ag(1)#3	82.00(11)	Ag(1)–Br(3)–Ag(1)#4	119.90(9)
Ag(1)#3–Br(3)–Ag(1)#4	68.16(18)		

Symmetry transformations used to generate equivalent atoms: #1 $-x + y + 1, -x + 1, z$; #2 $x, y, -z + 3/2$; #3 $-y + 1, x - y, z$; #4 $-y + 1, x - y, -z + 3/2$.

compatible to those found in Ag–Br compounds, $[Ph_4P]_2[(AgBr)_2(\mu\text{-}Br)_2]$ [28], $\{[(CH_3)_3S][Ag_2(\mu\text{-}Br)_2]\}_n$ [29], and $\{[Et_4N]_6[Ag_{12}Br_{18}]\}_n$ [30].

The solid-state structure of **2** has been confirmed by X-ray crystallography. A side view of $[(\mu_5\text{-}WSe_4)(AgBr)_5(\mu\text{-}Br)_2]^{4-}$ in **2** is shown in figure 2. Selected bond lengths and angles of **2** are given in table 3. The cluster consists of five AgBr fragments coordinated to five edges of the tetrahedral $[WSe_4]^{2-}$ along with two bridging halides connected to each of the two pairs of symmetric coppers, exhibiting a crown-like structure. The molecular structure possesses a crystallographic twofold axis passing through W(1), Ag(1) and Br(1). The tungsten has an approximately tetrahedral geometry with an average Se–W–Se angle of 108.77 (8)°. There are two types of W–Se bond lengths: the average of 2.3929(16) Å involving μ_4-Se is longer than that of 2.3393(18) Å involving μ_3-Se. The tetrahedral silvers are coordinated with one terminal bromide, one bridging bromide and two seleniums, while the trigonal silvers are bonded with one terminal bromide and two seleniums. Accordingly, the average Ag–Se bond length of 2.596(2) Å involving trigonal planar silver is slightly shorter than that of 2.687(2) Å involving tetrahedral silver. The average terminal and bridging Ag–Br bond lengths in **2** are 2.498(2) and 2.767(2) Å, respectively. The average

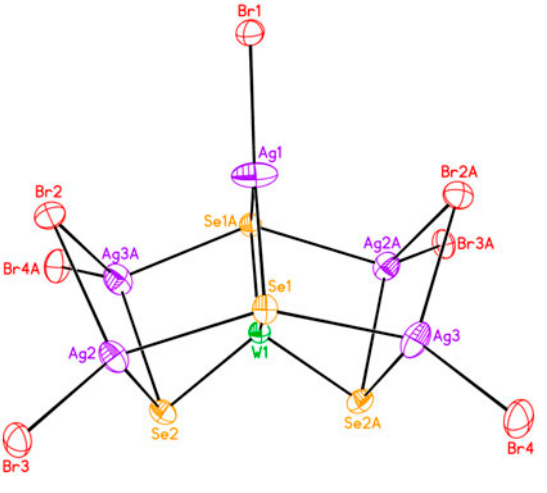

Figure 2. A perspective view of $[(\mu_5\text{-}WSe_4)(AgBr)_5(\mu\text{-}Br)_2]^{4-}$ in **2** with ellipsoids drawn at 40% probability.

Ag–Br–Ag bond angle is 74.93(6)° in **2**. The average W···Ag distance of 3.042(2) Å in **2** is comparable to those in [(μ_3-WSe_4)$Ag_3(PCy_3)_3$(μ_3-I)] (Cy = cyclohexyl) (av. 3.016(1) Å) and [(μ_3-WSe_4)Ag_3(μ_3-I)(μ-dppm)$_2$] (dppm = bis(diphenylphosphino)methane) (av. 2.992 (1) Å) [15].

The NLO properties of **2** were investigated by using the *Z*-scan technique [19]. The nonlinear absorption component was evaluated under an open aperture configuration. Theoretical curves of transmittance against the *Z*-position, equations (1) and (2),

$$T(Z) = \frac{1}{\pi^{1/2} q(Z)} \int_{-\infty}^{\infty} \ln[1 + q(Z)] e^{-\tau^2} \, d\tau \tag{1}$$

$$q(Z) = \alpha_2 I_i(Z) \frac{(1 - e^{-\alpha_0 L})}{\alpha_0} \tag{2}$$

were fitted to the observed *Z*-scan data by varying the effective third-order NLO absorptivity α_2 value, where experimentally measured α_0 (linear absorptivity), L (the optical path of sample), and $I_i(Z)$ (the on-axis irradiance at *Z*-position) were adopted. The solid line in figure 3(a) is the theoretical curve calculated with $\alpha_2 = 5.72 \times 10^{-9}$ m W^{-1} for 1.83×10^{-4} M in DMF. The non-linear refractive component of **2** was assessed by dividing the normalized *Z*-scan data obtained in the close-aperture configuration by those obtained in the open-aperture configuration. The nonlinear refractive component plotted with the filled squares in figure 3(b) was assessed by dividing the normalized *Z*-scan data obtained under the closed aperture configuration by the normalized *Z*-scan data obtained under the open aperture configuration. The valley and peak occur at equal distances from the focus. The difference in valley-peak positions ΔZ_{V-P} is 8.25 mm and the difference between normalized transmittance values at valley and peak positions ΔT_{V-P} is 3.17 mm for **2**. These

Table 3. Selected bond lengths (Å) and angles (°) for **2**. Estimated standard deviations are given in parenthesis.

W(1)–Se(1)	2.3929(16)	W(1)–Se(2)	2.3393(18)
Ag(1)–Se(1)	2.596(2)	Ag(2)–Se(1)	2.686(2)
Ag(3)–Se(1)	2.691(2)	Ag(2)–Se(2)	2.681(2)
Ag(3)–Se(2)#1	2.689(2)	Ag(1)–Br(1)	2.499(3)
Ag(2)–Br(2)	2.769(2)	Ag(2)–Br(3)	2.504(2)
Ag(3)–Br(4)	2.490(2)	Ag(3)–Br(2)#1	2.765(3)
W(1)···Ag(1)	2.974(2)	W(1)···Ag(2)	3.0730(15)
W(1)···Ag(3)	3.0799(16)		
Se(2)#1–W(1)–Se(2)	100.79(10)	Se(2)#1–W(1)–Se(1)	110.51(6)
Se(2)–W(1)–Se(1)	110.56(6)	Se(1)–W(1)–Se(1)#1	113.22(9)
W(1)–Se(1)–Ag(1)	73.07(6)	W(1)–Se(1)–Ag(2)	74.21(5)
W(1)–Se(1)–Ag(3)	74.31(6)	W(1)–Se(2)–Ag(2)	75.13(6)
W(1)–Se(2)–Ag(3)#1	75.19(6)	Ag(1)–Se(1)–Ag(2)	96.52(6)
Ag(1)–Se(1)–Ag(3)	96.24(7)	Ag(2)–Se(1)–Ag(3)	140.71(8)
Ag(2)–Se(2)–Ag(3)#1	77.63(7)	Se(1)#1–Ag(1)–Se(1)	100.65(10)
Se(2)–Ag(2)–Se(1)	92.89(7)	Se(2)#1–Ag(3)–Se(1)	92.57(7)
Br(1)–Ag(1)–Se(1)	129.68(5)	Br(3)–Ag(2)–Se(2)	122.94(8)
Br(3)–Ag(2)–Se(1)	120.41(8)	Se(2)–Ag(2)–Br(2)	103.50(7)
Se(1)–Ag(2)–Br(2)	101.01(7)	Br(4)–Ag(3)–Se(2)#1	121.10(9)
Br(4)–Ag(3)–Se(1)	117.00(9)	Se(2)#1–Ag(3)–Br(2)#1	103.39(7)
Se(1)–Ag(3)–Br(2)#1	101.29(7)	Br(3)–Ag(2)–Br(2)	112.34(9)
Br(4)–Ag(3)–Br(2)#1	117.23(10)	Ag(3)#1–Br(2)–Ag(2)	74.93(6)

Symmetry transformations used to generate equivalent atoms: #1 $-x + 1, y, -z + 3/2$.

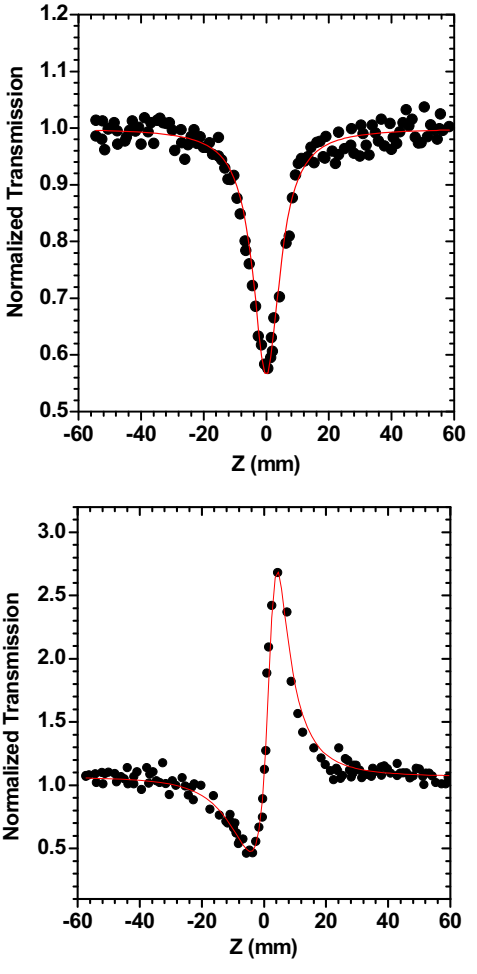

Figure 3. *Z*-scan data of 1.83×10^{-4} M of **2** in DMF at 532 nm with I_o being 9.21×10^{10} W m^{-2}: (a) collected under the open aperture configuration showing NLO absorption and (b) obtained by dividing the normalized *Z*-scan data obtained under the closed aperture configuration by the normalized *Z*-scan data in (a). The solid curves are theoretical fits based on *Z*-scan theoretical calculations.

results suggest an effective third-order optical nonlinearity [31]. The solid curve is an eye guide for comparison where the effective nonlinear refractivity n_2 value estimated is 3.64×10^{-9} esu for **2**. Comparing the NLO data of **2** with other reported argentoselenometallic clusters [9, 13–15, 32], the NLO behavior of **2** is comparable to those of polynuclear argentoselenometallic clusters. The positive value of nonlinear refraction in **2** indicates that there are self-focusing effects in NLO behavior of the present crown-like cluster compound, different from those of analogous crown-like copper clusters that show self-defocusing effects of nonlinear refraction [25]. This supports evidence that the structural alterations of clusters may give rise to variations in the NLO properties [10]. More examples of polynuclear argentoselenometallic clusters with novel structural types will be synthesized for investigation of the structure/NLO property relationship of these cluster compounds.

4. Conclusion

Two polynuclear homometallic and heterometallic clusters containing silver(I) bromide species have been synthesized and characterized by microanalytical and spectroscopic methods. Their molecular structures have been determined by single-crystal X-ray crystallography. The W–Se–Ag cluster compound $[Et_4N]_4[(\mu_5\text{-}WSe_4)(AgBr)_5(\mu\text{-}Br)_2]$ (**2**) exhibited nonlinear optical absorption and refraction as $\alpha_2 = 5.72 \times 10^{-9}$ m W^{-1} and $n_2 = 3.64 \times 10^{-9}$ esu, respectively, which are obviously stronger than those of analogous W–Se–Cu cluster compounds [25]. Such a significant improvement of non-linear absorption and refraction capability by replacing skeletal coppers with silvers implies the heavy atom effect [10]. Therefore, it may be a promising candidate for optical limiting materials compared to other related selenometallic clusters [8, 9]. More heteroselenometallic clusters with controlled structures and optical properties will be synthesized in the laboratory.

Supplementary material

Crystallographic data for $[Et_4N]_6[(AgBr)_6(\mu_3\text{-}Br)_2(\mu_3\text{-}Br)_3]Br$ (**1**) and $[Et_4N]_4[(\mu_5\text{-}WSe_4)(AgBr)_5(\mu\text{-}Br)_2]$ (**2**) have been deposited with the Cambridge Crystallographic Data Centre as supplementary publication Nos. CCDC 880554/880555, respectively. Copies of the data can be obtained free of charge on application to CCDC, 12 Union Road, Cambridge CB2 1EZ, UK [Fax: (+44)1233 336 033; E-mail: deposit@ccdc.cam.ac.uk].

Funding

This work was supported by the Natural Science Foundations of China [90301005], [21201003]; State Key Laboratory of Coordination Chemistry of Nanjing University.

References

[1] S. Shi, W. Ji, S.H. Tang, J.P. Lang, X.Q. Xin. *J. Am. Chem. Soc.*, **116**, 3615 (1994).
[2] H.W. Hou, X.Q. Xin, S. Shi. *Coord. Chem. Rev.*, **153**, 169 (1996).
[3] Y.Y. Niu, H.G. Zheng, H.W. Hou, X.Q. Xin. *Coord. Chem. Rev.*, **248**, 169 (2004).
[4] W. Ji, S. Shi, H.J. Du, P. Ge, S.H. Tang, X.Q. Xin. *J. Phys. Chem.*, **99**, 17297 (1995).
[5] G. Sankane, T. Shibahara, H.W. Hou, X.Q. Xin, S. Shi. *Inorg. Chem.*, **34**, 4785 (1995).
[6] J.P. Lang, K. Tatsumi, H. Kawaguchi, J.M. Lu, P. Ge, W. Ji, S. Shi. *Inorg. Chem.*, **35**, 7924 (1996).
[7] M.K.M. Low, H.W. Hou, H.G. Zheng, W.T. Wong, G.X. Jin, X.Q. Xin, W. Ji. *Chem. Commun.*, **4**, 505 (1998).
[8] Q.F. Zhang, W.H. Leung, X.Q. Xin. *Coord. Chem. Rev.*, **224**, 35 (2002).
[9] Q.F. Zhang, Y.N. Xiong, T.S. Lai, W. Ji, X.Q. Xin. *J. Phys. Chem.*, **B104**, 3476 (2000).
[10] S. Shi. In *Optoelectronic Properties of Inorganic Compounds*, D.M. Roundhill, J.P. Fackler Jr. (Eds.), pp. 55–105, Plenum Press, New York (1999).
[11] S.S. Yarovoi, A.I. Smolentsev, Y.V. Mironov. *J. Coord. Chem.*, **65**, 3998 (2012).
[12] J.Q. Wang, L. Weng, G.-X. Jin. *J. Organomet. Chem.*, **690**, 249 (2005).
[13] Q.F. Zhang, Z. Yu, J. Ding, Y. Song, A. Rothenberger, D. Fenske, W.H. Leung. *Inorg. Chem.*, **45**, 5187 (2006).
[14] Z. Yu, Q.F. Zhang, Y. Song, W.Y. Wong, A. Rothenberger, W.H. Leung. *Eur. J. Inorg. Chem.*, **15**, 2189 (2007).
[15] Q.F. Zhang, J. Ding, Z. Yu, Y. Song, A. Rothenberger, D. Fenske, W.H. Leung. *Inorg. Chem.*, **45**, 8638 (2006).
[16] S.C. O'Neal, J.W. Kolis. *J. Am. Chem. Soc.*, **110**, 1971 (1988).

[17] Bruker Analytical X-ray Instruments Inc. *SMART and SAINT+ for Windows NT (Version 6.02a)*, Bruker Analytical X-ray Instruments Inc., Madison, Wisconsin, USA (1998).
[18] G.M. Sheldrick. *SADABS*, University of Göttingen, Germany (1996).
[19] G.M. Sheldrick. *SHELXTL Software Reference Manual (Version 5.1)*, Bruker AXS Inc., Madison, Wisconsin, USA (1997).
[20] G.M. Sheldrick. *Acta Crystallogr.*, **A64**, 112 (2008).
[21] M. Sheik-Bahae, A.A. Said, T.H. Wei, D.J. Hagan, E.W. Van Stryland. *IEEE J. Quantum Electron.*, **26**, 760 (1990).
[22] M. Sheik-Bahae, A.A. Said, E.W. Van Stryland. *Opt. Lett.*, **14**, 955 (1989).
[23] H.W. Hou, B. Liang, X.Q. Xin, K.B. Yu, P. Ge, W. Ji, S. Shi. *J. Chem. Soc., Faraday Trans.*, **92**, 2343 (1996).
[24] T. Xia, A. Dogariu, K. Mansour, D.J. Hagan, A.A. Said, E.W. Van Stryland, S. Shi. *J. Opt. Soc. Am.*, **B15**, 1497 (1998).
[25] S. Miao, Z. Yu, Q.F. Zhang, Y. Song, A. Rothenberger, W.H. Leung. *J. Cluster Sci.*, **17**, 495 (2006).
[26] A. Müller, E. Diemann, R. JostesH. Bögge. *Angew. Chem., Int. Ed. Engl.*, **20**, 934 (1981).
[27] Y. Zhao, W. Su, R. Cao, M. Hong. *Acta Crystallogr.*, **C55**, ICU9900122 (1999).
[28] G. Helgesson, S. Jagner. *J. Chem. Soc., Dalton Trans.*, 2117 (1988).
[29] L.V. Shirshova, I.P. Lavrentev, V.I. Ponomarev. *Koord. Khim.*, **15**, 1048 (1989).
[30] G. Helgesson, S. Jagner. *Acta Crystallogr.*, **C44**, 2059 (1988).
[31] D.G. Mclean, R.L. Sutherland, M.C. Brant, D.M. Brandelik, P.A. Fleity, T. Pottenger. *Opt. Lett.*, **18**, 858 (1993).
[32] W.R. Yao, Y.L. Song, X.Q. Xin, Q.F. Zhang. *J. Mol. Struct.*, **655**, 79 (2003).